Appl. Phys. A (2014) 116:2007–2010
DOI 10.1007/s00339-014-8386-3

Applied Physics A
Materials Science & Processing

High dielectric constant nickel-doped titanium oxide films prepared by liquid-phase deposition

Ming-Kwei Lee · Chih-Feng Yen · Cho-Han Fan

Received: 19 November 2013 / Accepted: 11 March 2014 / Published online: 25 March 2014
© The Author(s) 2014. This article is published with open access at Springerlink.com

Abstract The electrical characteristics of nickel-doped titanium oxide films prepared by liquid-phase deposition on p-type (100) silicon substrate were investigated. The aqueous solutions of ammonium hexafluorotitanate and boric acid were used as precursors for the growth of titanium oxide films and the dielectric constant is 29. The dielectric constant can be improved to 94 by nickel doping at the thermal annealing at 700 °C in nitrous oxide.

1 Introduction

Titanium oxide (TiO_2) has the properties of high refractive index, excellent transmittance in the visible and near-infrared bands, and high electrical and chemical stability. It has been applied extensively to optoelectronic devices such as high-temperature optical filters, antireflection coatings, solar energy converters, and optical waveguides [1–3]. TiO_2 can also be used as the dielectric material of the storage capacitor in dynamic random access memory (DRAM) and high-k gate dielectric of MOSFET because of its high dielectric constant [4, 5].

There are many methods for the growth of TiO_2 film, such as sol–gel, magnetron sputtering, metal organic chemical vapor deposition, liquid-phase deposition (LPD), and, etc. [6, 7]. Liquid-phase deposition has many advantages such as high uniformity, good selectivity, mass production capability, conformal growth and low cost [8]. The structure of as-deposited LPD-TiO_2 is amorphous prepared at the near room temperature, but its dielectric constant is as low as about 4.7 [9]. The dielectric constant of LPD-TiO_2 can be much improved by high-temperature thermal annealing from the formation of anatase and rutile phases. Usually, the anatase phase of TiO_2 will be formed in the temperature range of 400–800 °C and transformed into higher dielectric constant rutile phase at the temperature higher than 900 °C [10]. For LPD-TiO_2, the dielectric constant of anatase phase is 29.5 at the thermal annealing of 450 °C [11]. The rutile phase LPD-TiO_2 is formed at the thermal annealing of 900 °C in this study. Such a high thermal annealing temperature will induce wafer warpage, doping redistribution, the inter-diffusion at interface and, etc.

Ni-doped TiO_2 were wildly investigated currently [12–16]. From a previous study [14], the annealing temperature for anatase–rutile transformation can be lowered by nickel (Ni) doping. Due to the local charge imbalance with the incorporation of Ni into TiO_2, the generated oxygen vacancy can enhance atom migration to form the rutile phase. In this study, the crystallization and electrical characteristics of Ni-doped LPD-TiO_2 films grown on p-type (100) silicon substrate were investigated.

2 Experimental procedure

Boron-doped, p-type (100)-oriented silicon wafer with a resistivity of 15–25 Ω-cm was used as the substrate in this experiment. Ammonium hexafluorotitanate ($(NH_4)_2TiF_6$) and boric acid (H_3BO_3) aqueous solutions were used as

M.-K. Lee
Department of Electronic Engineering, Chung Yuan Christian University, Chung Li 32023, Taiwan, Republic of China

C.-F. Yen (✉)
Department of Materials Science and Engineering, MingDao University, Chang Hua 52345, Taiwan, Republic of China
e-mail: cfyen@mdu.edu.tw

C.-H. Fan
Department of Electrical Engineering, National Sun Yat-sen University, Kaohsiung 80424, Taiwan, Republic of China

precursors for the growth of LPD-TiO_2. For the growth of undoped TiO_2 film, 20 ml of 0.2 M $(NH_4)_2TiF_6$ and 20 ml of 0.4 M H_3BO_3 were mixed as the growth solution. For the preparation of 0.2 M $(NH_4)_2TiF_6$, 19.8 g of $(NH_4)_2TiF_6$ was added into 500 ml deionized (DI) water and stirred steadily for 16 h at room temperature. For the preparation of 0.4 M H_3BO_3, 12.6 g H_3BO_3 was mixed with 500 ml DI water. The growth temperature was kept at 40 °C. For Ni doping, 5 ml saturated nickel chloride solution was added in the growth solution. The saturated nickel chloride solution was prepared by dissolving 118.8 g of $NiCl_2{\cdot}6H_2O$ powder into 500 ml DI water at room temperature. There is a high concentration of oxygen vacancy in as-grown LPD-TiO_2 film. Oxygen vacancy is the typical defect in LPD-TiO_2 film [17]. Moreover, LPD-TiO_2 has more concentration oxygen vacancy than that by other deposition methods (sol–gel, magnetron sputtering and metal organic chemical vapor deposition) due to high concentration of water molecules examined by FTIR in LPD-TiO_2 film [9]. The oxygen vacancy can be removed efficiently by oxygen atom provided in N_2O thermal annealing [18]. For the formation of anatase and rutile phases and reduction of oxygen vacancy of as-deposited undoped and doped LPD-TiO_2 films, N_2O was used as the treatment ambient in thermal annealing.

Scanning electron microscope (SEM) was used to measure the film thickness. X-ray was used to examine the crystalline structure. Chemical bonding was analyzed with X-ray photoemission spectroscopy (XPS). The capacitance–voltage characteristics were measured with Agilent E4280A meter at the frequency of 1 MHz with 30-mV signal amplitude.

3 Results and discussion

Smooth undoped and Ni-doped LPD-TiO_2 films grown on Si were obtained. The thicknesses of undoped and Ni-doped LPD-TiO_2 films as a linear function of the deposition time at the deposition temperature of 40 °C are shown in Fig. 1. The growth rates are 42.7 and 40.1 nm/h, respectively. The thicknesses of TiO_2 films were measured by SEM. Therefore, a quite low measurement error for the growth rate of about 5 % can be obtained. The repeatability is quite high and the run to run error is about 10 %. The slightly lower growth rate with Ni doping could be from the hindrance of Cl_2 molecules. The XPS of thermally annealed Ni-doped LPD-TiO_2 film at 700 °C is shown in Fig. 2. Carbon is from the surface contamination. The weak Ni peaks shown in the inset indicate the successful Ni doping. The concentration is estimated to be about 300 ppm. Ni dopant concentration can be controlled by modulating the volume of saturated nickel chloride solution in the growth solution.

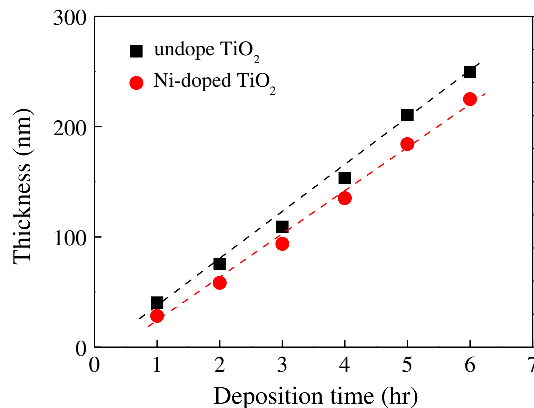

Fig. 1 Thickness of undoped and Ni-doped LPD-TiO_2 films as a linear function of the deposition time at the deposition temperature of 40 °C

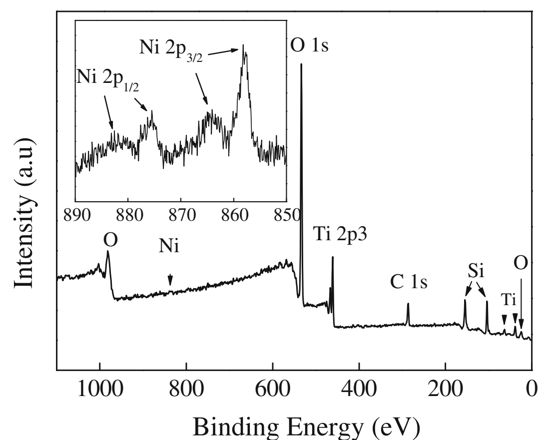

Fig. 2 X-ray photoelectron spectroscopy of annealed Ni-doped LPD-TiO_2

The X-ray diffraction spectra of as-deposited and annealed Ni-doped LPD-TiO_2 films in the range of 600–900 °C are shown in Fig. 3. The structure of as-deposited TiO_2 is amorphous. The low signal-to-noise ratio indicates that TiO_2 nanoparticles are contained in an amorphous matrix. The TiO_2 anatase phase with the orientations of (101), (112) and (200) is observed at the annealing temperature of 600 °C and decreases with the annealing temperature [19]. The TiO_2 rutile phase with the orientation of (002) is observed at the annealing temperature of as low as 700 °C from the generation of oxygen vacancy by the replacement of Ti by Ni [14, 20]. The intensity of rutile phase increases at 800 °C and then decreases slightly at 900 °C, because of the high replacement of Ti by Ni and partial destruction of Ti–O (bond length of 1.972 Å [22]) rutile phase [23] by the shorter Ni–O bond length of 1.77 Å [21]. The anatase phase disappears at 900 °C from the complete transformation into the rutile phase.

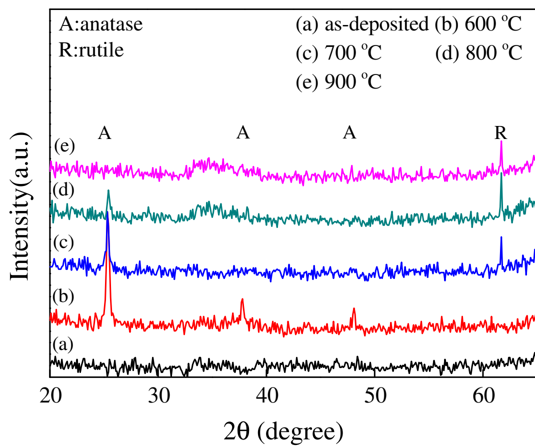

Fig. 3 XRD spectra of annealed Ni-doped LPD-TiO_2 films in the range of 600–900 °C

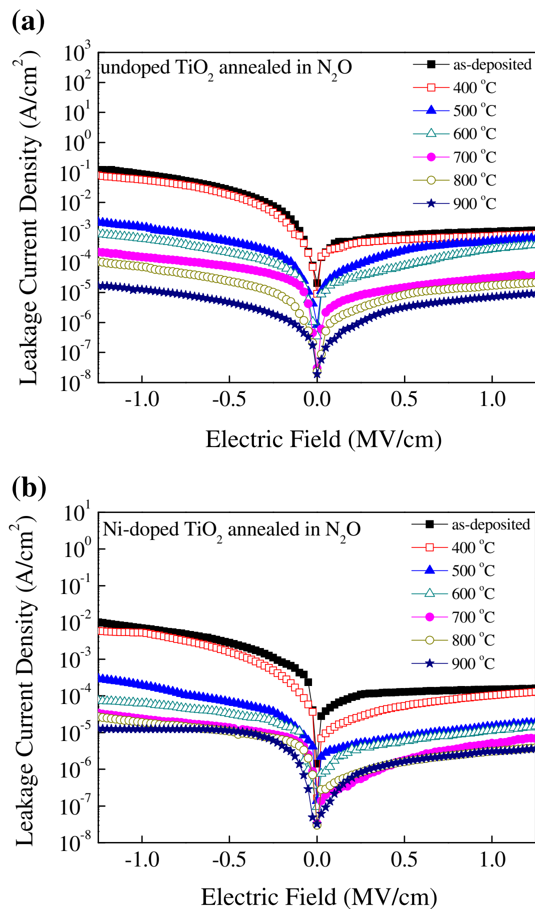

Fig. 4 **a** I–V characteristics of undoped LPD-TiO_2 films as a function of annealing temperature. **b** I–V characteristics of Ni-doped TiO_2 films as a function of the annealing temperature

The leakage current densities of as-deposited and annealed samples undoped LPD-TiO_2 films with a fixed thickness of 220 nm are shown in Fig. 4a. The high

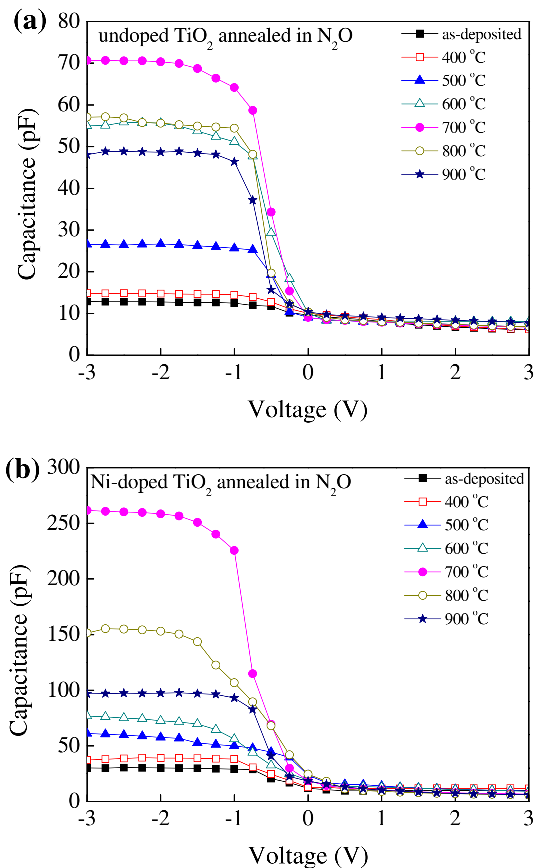

Fig. 5 **a** C–V characteristics of undoped LPD-TiO_2 films as a function of annealing temperature. **b** C–V characteristics of Ni-doped TiO_2 films on Si as a function of the annealing temperatures

leakage current density of as-deposited LPD-TiO_2 film is from oxygen vacancies. After N_2O annealing, the leakage current density decreases with the annealing temperature from the decrease of oxygen vacancy. For the annealing temperature from 400 to 700 °C, the leakage current densities are improved from 8.84×10^{-4} and 7.65×10^{-2} A/cm^2 to 3.69×10^{-5} and 2.23×10^{-4} A/cm^2 at ±1.25 MV/cm, respectively. The further decrease of leakage current density at the annealing temperature higher than 800 °C is due to the formation of SiO_2 at the TiO_2/Si interface [24], which is supported by the following C–V characterization.

The I–V characteristics of Ni-doped TiO_2 films as a function of the annealing temperature in N_2O are shown in Fig. 4b. The leakage current density of as-deposited Ni-doped film is lower than that of as-deposited undoped film. It is because the stoichiometry of NiO is usually metal deficient and the excess oxygen will compensate the oxygen vacancy of TiO_2 [25]. The leakage currents are improved to 6.88×10^{-6} and 3.39×10^{-5} A/cm^2 at ±1.25 MV/cm at the annealing temperature of 700 °C. The leakage current is improved slightly for the annealing

Table 1 *k* values of undoped and doped films as a function of annealing temperature

Annealing temperature (°C)	400	500	600	700	800	900
Undoped films *k* values	6	11	23	29	23	20
Doped films *k* values	14	21	27	94	56	35

temperature higher than 800 °C from the formation of SiO_2 at the TiO_2/Si interface.

The C–V characteristics of undoped films as a function of annealing temperature were shown in Fig. 5a. The low accumulation capacitance of as-deposited TiO_2 film is from its amorphous structure and high leakage current. The capacitance increases with the annealing temperature due to the reduction of water molecules and hence the leakage current. It decreases at the annealing temperature higher than 800 °C from the formation of SiO_2 at interface. The *k* values are 6, 11, 23, 29, 23 and 20 from 400 to 900 °C.

The C–V characteristics of Ni-doped TiO_2 films as a function of the annealing temperature are shown in Fig. 5b. The accumulation capacitance of as-deposited amorphous TiO_2 film is larger than that of undoped one due to lower leakage current. The capacitance increases with the annealing temperature due to the reduction of oxygen vacancy. It decreases at the annealing temperature higher than 800 °C from the formation of SiO_2 at the TiO_2/Si interface. The *k* values are 14, 21, 27, 94, 56 and 35 at from 400 to 900 °C. From Fig. 3, the X-ray peak intensity of anatase phase is 600 > 700 °C, but the peak intensity of rutile phase at 600 °C is negligible. Therefore, the *k* value of Ni-doped TiO_2 film annealed at 700 °C is larger than that at 600 °C. The peak intensity of rutile phase is 800 > 700 °C, but that of anatase phase is 800 < 700 °C at a relatively larger extent. Therefore, the *k* value of Ni-doped TiO_2 film annealed at 700 °C is larger than that at 800 °C. From above discussion, the *k* value of Ni-doped TiO_2 film has a maximum at the annealing temperature of 700 °C.

To read more clearly, the *k* values of undoped and doped films as a function of annealing temperature are listed in Table 1.

4 Conclusions

In conclusion, the electrical characteristics of nickel-doped titanium oxide films prepared by liquid-phase deposition on p-type (100) silicon substrate were improved from the decrease of oxygen vacancy by the excess oxygen compensation of NiO. The dielectric constant of nickel-doped LPD-TiO_2 film can be improved to 94 at thermal annealing temperature of as low as 700 °C in nitrous oxide. It is from that the rutile phase formation for Ni-doped TiO_2 film is lower than that of undoped one from the oxygen vacancy generation by Ni doping.

Acknowledgments The authors would like to thank the National Science Council of Republic of China for their support under contract Nos. 98-2221-E110-073-MY3 and NSC101-3113-E-182-001-CC2.

Open Access This article is distributed under the terms of the Creative Commons Attribution License which permits any use, distribution, and reproduction in any medium, provided the original author(s) and the source are credited.

References

1. M.A. Butler, D.S. Ginley, J. Mater. Sci. **15**, 1 (1980)
2. T. Carlson, G.L. Griffin, J. Phys. Chem. **90**, 5896 (1986)
3. X.R. Wang, H. Masumoto, Y. Someno, T. Hirai, J. Jpn. Inst. Metals. **62**, 1069 (1998)
4. K. Vydianathan, G. Nuesca, G. Peterson, E.T. Eisenbraun, A.E. Kaloyeros, J.J. Sullivan, B. Han, J. Mater. Res. **16**, 1838 (2001)
5. J. Yan, D.C. Gilmer, S.A. Campbell, W.L. Gladfelter, R.G. Schmid, J. Vac. Sci. Technol. B. **14**, 1706 (1996)
6. M.K. Lee, C.F. Yen, J.J. Huang, S.H. Lin, J. Electrochem. Soc. **153**, 266 (2006)
7. M.K. Lee, J.J. Huang, C.M. Shih, C.C. Cheng, Jpn. J. Appl. Phys. **41**, 4689 (2002)
8. T.J. Richardson, M.D. Rubin, J. Electrochem. Soc. **46**, 2119 (2001)
9. M.K. Lee, B.H. Lei, Jpn. J. Appl. Phys. **39**, L101 (2000)
10. J.G. Yu, H.G. Yu, B. Cheng, X.J. Zhao, J.C. Yu, W.K. Ho, J. Phys. Chem. B. **107**, 13871 (2003)
11. M.K. Lee, H.C. Lee, C.M. Hsu, Mater. Sci. Semicond. Process. **10**, 61 (2007)
12. K. Karthick, S. Kesavapandian, N. Victor Jaya, Appl. Surf. Sci. **256**, 6829 (2010)
13. M. Dhayal, S.D. Sharma, C. Kant, K.K. Saini, S.C. Jain, Surf. Sci. **602**, 1149 (2008)
14. K.S. Hwang, J.H. Jeong, J.H. Ahn, B.H. Kim, Ceram. Int. **32**, 935 (2006)
15. V. Rodríguez-González, M.A. Ruiz-Gómez, L.M. Torres-Martínez, R. Gómez, Top. Catal. **54**, 490 (2011)
16. S.D. Sharma, D. Singh, K.K. Saini, C. Kant, V. Sharma, S.C. Jain, C.P. Sharma, Appl. Catal. A **314**, 40 (2006)
17. J. Strunk, W.C. Vining, A.T. Bell, J. Phys. Chem. C **113**, 16937 (2010)
18. S.C. Sun, T.F. Chen, Tech. Dig. Int. Electron Devices Meet. 333 (1994)
19. J. Liqiang, S. Xiaojun, C. Weimin, X. Zili, D. Yaoguo, F. Honggang, J. Phys. Chem. Solids **64**, 615 (2003)
20. N.H. Hong, J. Sakai, W. Prellier, J. Magn. Magn. Mater. **281**, 347 (2004)
21. H. Peng, J. Li, S.S. Li, J.B. Xia, J. Phys. Chem. C **112**, 13964 (2008)
22. G. Kleinle, J. Wintterlin, G. Ertl, R.J. Behm, F. Jona, W. Moritz, Surf. Sci. **225**, 171 (1990)
23. Y. Wang, L. Zhang, J. Phys. Chem. C **113**, 9210 (2009)
24. M. Kadoshima, M. Hiratani, Y. Shimamoto, K. Torii, H. Miki, S. Kimura, T. Nabatame, Thin Solid Films **424**, 224 (2003)
25. P. Kofstad, Oxid. Met. **44**, 3 (1995)